Out-of-focus holography at the Sardinia Radio Telescope

F. Buffa[a], G. Serra[b], S. Poppi[a], E. Egron[a], M. Murgia[a], and A. Pinna[c]

[a]INAF, Osservatorio Astronomico di Cagliari, Via della Scienza 5, 09047 Selargius (CA), Italy
[b]Agenzia Spaziale Italiana, COT-Direzione Coordinamento Tecnico-Scientifica, Sede ASI Cagliari, Via della Scienza 5, 09047 Selargius (CA), Italy
[c]CRS4 - Centro di Ricerca, Sviluppo e Studi Superiori in Sardegna, Loc. Piscina Manna, 09050 Pula (CA), Italy

ABSTRACT

We present here the results of an OOF holography campaign recently performed at the SRT observing a high flux density radio source as the W3(OH) water maser by using the K-band 7 feeds Focal Plan Array receiver centered at 22.23 GHz. The resulting OOF maps (0.2 times 0.2 deg extent) of the SRT radiation pattern allowed to retrieve the gravitational large scale deformation on the aperture plane at 65 deg elevation.

Keywords: Large telescope, reflector surface measurement, Out-Of-Focus holography

1. INTRODUCTION

The Sardinia Radio Telescope (SRT) is a general purpose fully steerable 64 m diameter radio telescope designed to operate with high efficiency within the 0.3-116 GHz frequency range.[1] Since December 2018 the telescope has been opened to the international community to carry out radio astronomy observing programs using an initial set of cryogenic receivers hosted in three different focal positions (primary, gregorian and beam wave guide foci) covering four radio frequency bands in the 0.3-26.5 GHz range. The SRT operates in single-dish (continuum, full Stokes and spectroscopy), Very Long Baseline Interferometry (VLBI) and Space Science modes and it has been successfully used also for space-debris detection and Sun observations (see Science with SRT).

The telescope optical design is based on a quasi-Gregorian configuration with two shaped (a 64m diameter primary or M1, and a 7.9 m diameter secondary or M2) mirrors which, working together, minimize the spillover and the standing waves of the antenna, mainly during gregorian and beam wave guide observations. An active surface (AS), composed by 1008 aluminium panels shifting along vertical direction, thanks to 1116 electro-mechanical actuators, together with 6 electro-mechanical actuators behind M2, allow a real-time compensation for the gravitational deformations affecting M1 shape and the M1-M2 axis misalignment varying with the elevation. In addition, the AS can move from a shaped tabulated profile to a parabolic profile for primary focus band observations.

In the last few years, we have successfully commissioned and tested a primary focus holographic system[2] for the SRT. Based on the phase-coherent microwave holography technique, the system can measure the SRT far-field pattern at 11.5 GHz and correct the primary mirror deformations with high spatial resolution and good accuracy at two antenna elevation angles (30 and 44 deg), where the geosynchronous satellites are available at the telescope latitude.

Recently, we decided to extend the analysis to the entire elevation range by implementing the Out-Of-Focus holography (OOF), a phase-retrieval technique, proposed by B. Nikolic et al.[3] , being routinely used in many single-dish facilities. In this approach, the telescope aperture field phase is retrieved by measuring three antenna far-field maps (i.e. an OOF data set), one in-focus and the other two got by symmetrically defocusing the sub-reflector, in a standard astronomy observations set-up and, then, implementing a fitting algorithm based on Zernike polynomials. In our case, we preferred the k-band dual polarization cryogenic receiver, a 7-beams focal plane array (FPA) hosted in the SRT Gregorian turret, which can be automatically moved on the gregorian

Further author information: (Send correspondence to S. Poppi)
S. Poppi.: E-mail: sergio.poppi@inaf.it

Ground-based and Airborne Telescopes VIII, edited by Heather K. Marshall, Jason Spyromilio, Tomonori Usuda, Proc. of SPIE Vol. 11445, 114456G · © 2020 SPIE
CCC code: 0277-786X/20/$21 · doi: 10.1117/12.2561787

focus, allowing to operate in the frequency range 18-26.5 GHz, the SRT highest frequency range to date. In this way we can receive both astronomical sources (high flux density calibrator or water-maser) and 21 GHz geostationary satellite signals, so extending widely the elevation angular range at which performing holographic measurements.

In Section 2 we describe the changes the authors made in the OOF software package to process a SRT far-field data set. In Section 3 the result of a typical OOF processing of a data set, recorded pointing SRT to the W3(OH) water maser, at 22.23 GHz are presented. Such a result, i.e. the deformation map on the SRT aperture plane, is then compared to the deformation map measured by close range photogrammetry almost at the same telescope angular elevation. Finally, summary and conclusions are reported in Section 4.

2. SHAPED SURFACES ANALYSIS: RAY-TRACING AND IMPLEMENTATION

The original OOF algorithm, developed by Nikolic et al., was recently ported in Python by T. Cassanelli. The Cassanelli's software, `pyoof`, is distributed on GitHub. The Cassanelli's `pyoof` code was deeply revised and adapted to the SRT geometry and optical configuration. The major changes concern the effect of the extra path, due to the defocus, resulting in the field phase on the SRT aperture plane. In facts, the SRT M1 reflector is a rotational symmetry surface generated by a shaped radial parabolic curve which can only be described in terms of a tabulated profile, significantly different (a few cm) from a standard parabolic one (see Fig. 1) with respect to the SRT minimum wavelenght (3 mm).

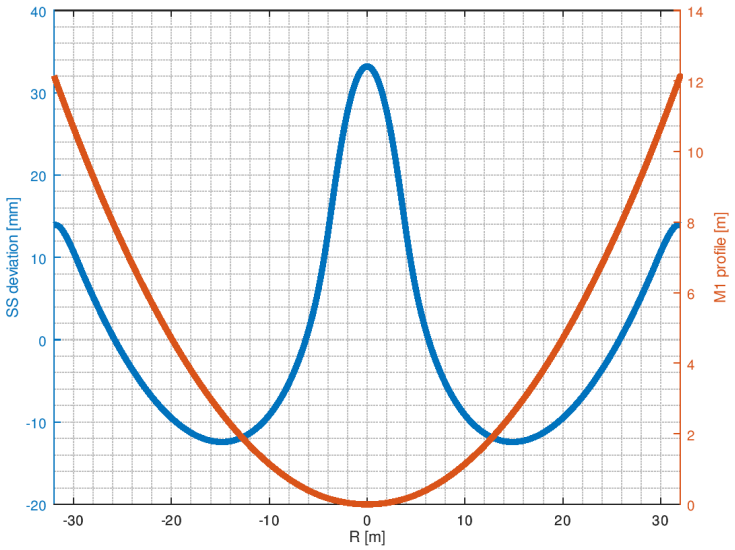

Figure 1. Shaped radial parabolic profile of the SRT primary reflector (red, right scale) and deviation from the standard parabolic profile (blue, left scale).

For standard Cassegrain and Gregorian radio telescopes the extra phase contribution due to the M2 axial defocussing Δz is

$$\delta(x, y, \Delta z) = \Delta z \left(\frac{1 - a^2}{1 + a^2} + \frac{1 - b^2}{1 + b^2} \right) \frac{2\pi}{\lambda}, \tag{1}$$

where λ is the wavelength, $a = R/2f$, $b = R/2F$ and $R = \sqrt{x^2 + y^2}$ is the radius of the aperture plane, while f and F are the focal length of the primary reflector and the effective total focal length, respectively.

Jian et al. have recently reported[4] that Equation (1) cannot be directly used in the out-of-focus algorithm for processing data set recorded by means of an antenna equipped with shaped reflectors. The extra phase can be only evaluated by ray-tracing the extra path due to the sub-reflector displacement Δz long the telescope axis

(z-axis). In Fig. 2 we show the geometric extra paths corresponding to $\Delta z = -0.027\ m$, i.e. the axial translation, we commanded the SRT sub-reflector to acquire the two out-of-focus far-field maps, calculated for a standard

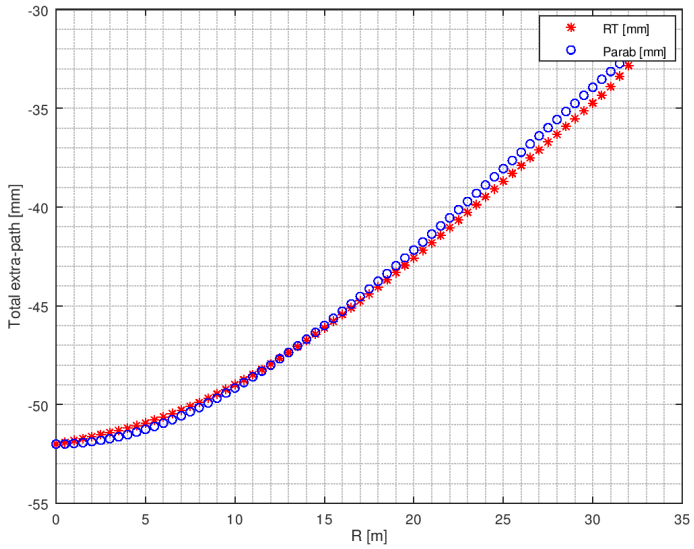

Figure 2. Geometric extra paths corresponding to a $\Delta z = -0.027\ m$ defocussing, i.e. 2λ at 22.23 GHz, for a standard parabolic profile (blue circles, Parab) and for SRT case as obtained by the ray-tracing procedure (red stars, RT).

parabolic profile by applying Equation (1) and for the SRT shaped profile by the ray-tracing procedure (RT). Since the ray-tracing implementation turns out to be extremely time-consuming in the OOF fitting running, we have chosen to calculate the extra path contribution in advance and to parameterize it in function of R and Δz. In this way, the extra path contribution, due to the shaped surface profile may be considered as a correction factor to the standard case. The correction factor may be evaluated for a representative number of different configurations and then parameterized by a bi-variate polynomial fitting, where R, the radial distance from the antenna axis and Δz are the variables. In Fig. 3 we show the correction factor calculated by the RT ray-tracing procedure (RT) and the corresponding polynomial fitting (Poly). The fitting maximum error turned out to be equal to $20\mu m$ RMS. The polynomial coefficients have been then hard-coded in the `pyoof` fitting routine after multiplying the geometric extra path by $2\pi/\lambda$ to get the extra phase contribution on the antenna aperture field.

3. OOF-PHOTOGRAMMETRY COMPARISON

In this section we present the result of the OOF analysis of a SRT k-band far-field dataset recorded in April 2019 during a daytime telescope allocation addressed to the AS calibration experiments. During this experiment the telescope was set to observe the radio source W3(OH), a water maser having a high flux density (usually more than 1000 Jy) radio emission in a narrow band (a few hundred kHz) around 22.23 GHz. All the 14 signals coming from the 7 FPA feeds (each one receiving two polarizations) were recorded, while a standard on-the-fly (OTF) azimuth scan observation strategy was carried out to acquire three OOF maps. Each map 0.2 deg * 0.2 deg extent was composed by 49 azimuth scans, one separated from the other along the elevation direction of about one third of the SRT half power beam width (0.015 deg @ 22.23 GHz). The data set (three maps) acquisition lasted about 45 minutes (15 minutes for each map and about 18 s per each scan), in the meanwhile the water maser moved of about 2 deg from 64 to 66 degree in elevation. Two of the three OOF maps were recorded by running a telescope schedule such that an on-axis displacement Δz of the sub-reflector was set before starting the on-the-fly scan, kept for the whole map acquisition and deleted at the end of the acquisition. This telescope defocusing Δz was equal to -2λ for one map (the sub-reflector moved away from the main reflector) and 2λ for the second map (the sub-reflector moved toward the main reflector), with $\lambda = 13.5$ mm at 22.23 GHz.

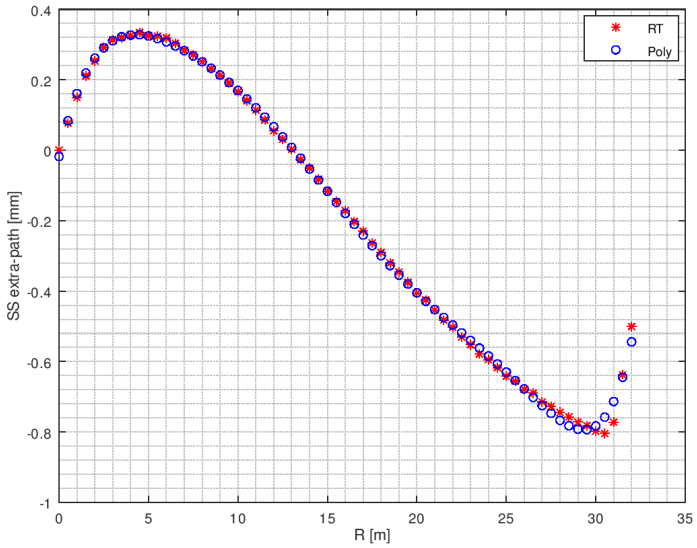

Figure 3. Geometric shaped surface (SS) contribution to the extra path due to a defocussing equal to $\Delta z = -0.027\ m$. Such term is added to the extra path expressed by Equation (1) in order to calculate the full defocussing effect. Red stars represent the SS contribution as evaluated by the ray-tracing, while the blue circles are the corresponding polynomial fitting.

The frequency of the receiver local oscillator was chosen equal to 21588 MHz in order to frequency down-convert the W3(OH) signal spectrum in a suitable position (with central frequency in 642 MHz) of the SRT intermediate frequency (IF) base band (BB) ($100 - 2100\ MHz$). During each map acquisition, a 1500 MHz-band of the IF signal was digitalized and measured every 30 ms by the Sardara backend,[5] setting the maximum number of the frequency channels (16384) with a resulting frequency resolution equal to 92 kHz.

The experiment was performed around 65° elevation, keeping the sub-reflector in a tracking mode on the source to ensure the correct antenna pointing and the main reflector active surface (AS) parked. As a consequence, the AS was not correcting for gravitational deformations and we were able to perform our experiment addressed to retrieve the effect of such surface misalignment by oof holography technique. For this reason the in-focus far-field maps (see Fig. 4) are affected by coma and other minor optical aberrations due even to the slight misalignment between the axes of M1 and M2 reflectors.

It is worth to noting that only the data set related to the right-hand (RH-) and left-hand (LH-) circular polarizations (CP) received by the central feed of the k-band FPA were used to process the SRT far-field pattern maps by the OOF software. In fact, this latter still does not include a routine to process a multi-feed data set.

In Fig. 4 the comparison between the measured SRT far-field pattern maps (first row) and the related pattern maps (second row) resulting from the OOF fitting shows a good agreement, as one can be seen especially in the representation of the coma aberration in the in-focus pattern map (see central column).

The signal to noise ratio (SNR) reached during the in-focus map was equal to 21 dB, certainly lower than the value we expect with the AS set on active mode and if we had performed the measurement during nighttime. We estimate a SNR drop of about 7 dB: 5 dB due to the fact that M1 was not correcting for gravitational deformation and 2 dB due to a system temperature value equal to 130 K, almost 50 K greater than the optimal one, about 80 K, the k-band FPA receiver usually measures during nighttime and low sky opacity. However, this is not a critical issue for this preliminary OOF experiment at SRT. In fact, this experiment was thought to allow a comparison between the deformation map resulting from the OOF measurements here presented and that deriving from the photogrammetry campaign[6] performed in 2012 during the SRT commissioning phase.

Table 1. Summary of the receiver settings and OOF observing strategy parameters chosen during the SRT measurement in April 2019

Radio source			
Name	Flux density [Jy]	Freq [GHz] ($\lambda[mm]$)	Freq band [kHz]
W3(OH)	> 1000	22.23 (13.5)	a few hundred
Radio source			
Type	Feeds	Freq band [GHz]	Polarization
k-band FPA	7	18-26.5	RHCP and LHCP
M1 AS and M2 settings			
M1 Profile	M1 actuators	M2 actuators	Defocus Δz [mm]
Shaped	parked	active	± 27
Observation parameters			
HPBW [deg]	elevation [deg]	Tsys [K]	SNR [dB]
0.015 @ 22.23 GHz	65	130	21
Receiver settings			
LO freq [MHz]	Filter band [MHz]	W3(OH) CF @ IF[MHz]	BB [MHz]
21588	1500	642	100-2100
Digital backend settings			
Type	Channels	spectral resolution [kHz]	Integration time [ms]
spectro-polarimeter	16384	92	30
Observing strategy			
map size [deg^2]	az scan separation [deg]	scan time [s]	map time [min]
$0.2 * 0.2$	0.004 ($\sim$ 0.28 HPBW)	18	~ 15

For sake of the simplicity of the reading, we have summarized receiver settings and the OOF observing strategy parameters in Table 1.

Hereafter, we show, in particular, the comparison between the map of the surface deformations measured at 65° by OOF method (Fig. 5) and the map of the surface deformations measured by the close range photogrammetry at 60° (Fig. 6). In both cases the SRT AS was set in parking mode.

Such a comparison has to take into account the intrinsic differences between the two methods. First of all, the OOF method measures the sum of the deformations and the misalignment of the SRT main and secondary reflectors. Instead, the photogrammetry measured only the SRT main reflector surface deformations. The first one is an inverse method, whose spatial resolution is relatively poor (in our case we estimate a pixel size of about $\simeq 14\ x\ 14$ sqm); conversely, the photogrammetry is a direct method whose accuracy is imposed by the camera *internal* and *external* parameters and whose spatial resolution depends, ultimately, by the target arrangement

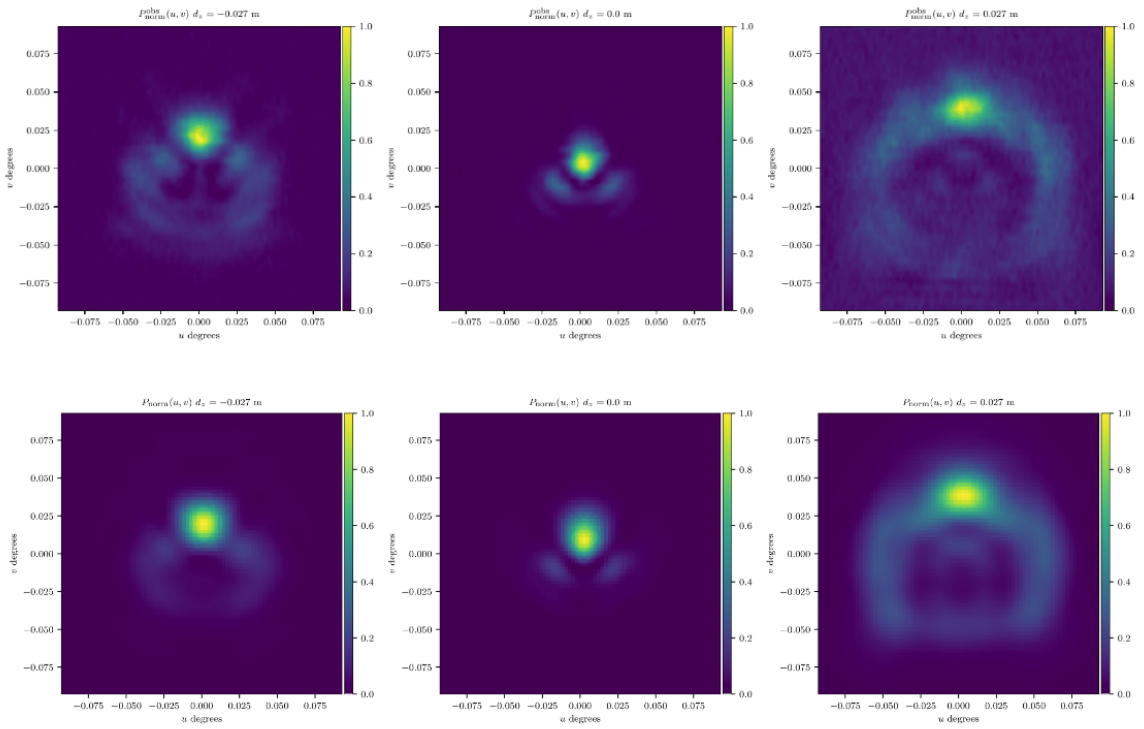

Figure 4. Measured (top) and fitted (bottom) pattern maps, from left to right: $\delta z = -2\lambda$, $\delta z = 0$ and $\delta z = +2\lambda$.

($\simeq 1.7\ x\ 1.7$ sqm in the 2012 measurement). That said, the two maps, taken at close elevation angles, show similar large scale surface deformations, having almost the same position and amount. The deformations retrieved by the OOF technique are consistent with the action of gravitational loads on the SRT main reflector, except for a scale factor (in the interval between 1 and 2) to be still define. Moreover, it is worth to noting that the OOF map is much more affected by noise, mainly in the reflector upper outer rings, due to the fact the measurement were performed during the daytime and in a not nominal optical configuration: the AS was parked and, as consequence, an antenna gain drop was unavoidable.

4. DISCUSSION AND CONCLUSIONS

In this paper we have described the changes needed to make the standard OOF package (`pyoof`) compatible with the processing of a far field pattern data sets measured at SRT. We have calculated in advance the extra path in the out-focus-maps due to the shaped profile by a polynomial fitting and added to the OOF software routine. Then, we have analyzed a SRT OOF dataset measured in April 2019 pointing the telescope to the water maser W3(OH). We have discussed the results and compared them to those we got by means of close range photogrammetry in 2012 at a close elevation angle. This comparison has shown that the version of `pyoof` adapted to the SRT case produces results consistent with the "real" gravitational large scale deformations, despite of the noisy data set recorded during a daytime measurement session which affected the resulting SNR on the OOF maps.

New experiments will be soon scheduled at the SRT with the nominal optical configuration, i.e. with M1 and M2 in the active mode, with the aim to perform a fine calibration of the current M1 AS look-up table. The next measurement will be preferably carried out in a suitable nighttime session, to minimize the system noise temperature, and, if needed, increasing the integration time in order to improve the OOF map signal-to-noise ratio. In addition, a stable high flux radio astronomical calibrator, emitting a broad frequency band signal, will be evaluated as an alternative to the water maser.

Finally, we hope to be able soon to test the OOF software with a full multi-beam dataset. A multi beam

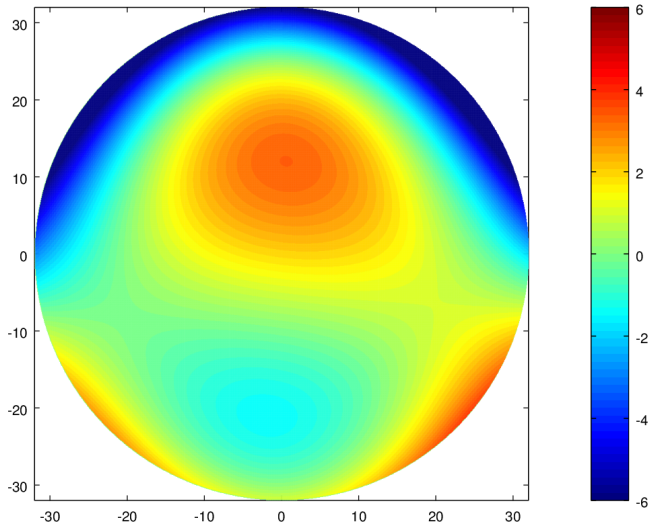

Figure 5. OOF deformation map [mm] at elevation equal to 65°.

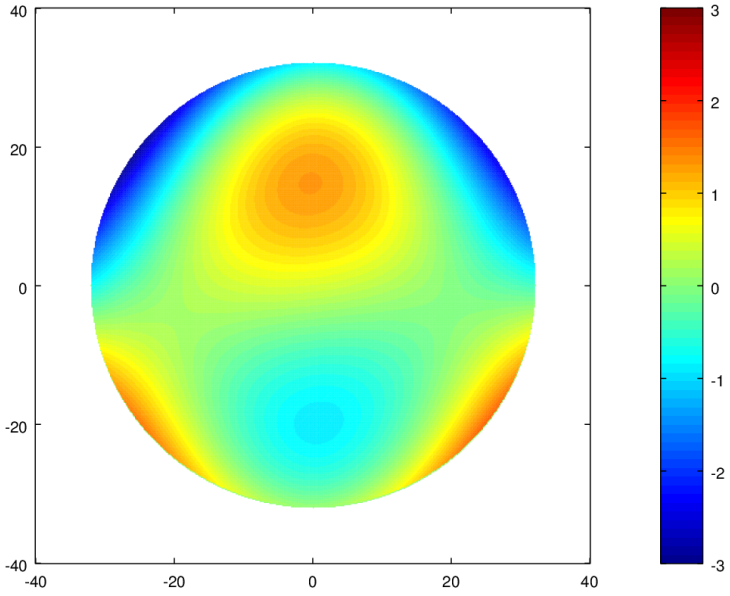

Figure 6. Close range photogrammetric map [mm] at elevation equal to 60°. A smoothing with a high order Zernike polynomial fitting was applied.

observation with a suitable observation strategy would improve the signal-to-noise ratio thanks to a greater exposition of the feeds to the radio source and would also make the acquisition of the far-field pattern data set significantly faster, allowing to measure even the large scale deformations due to thermal gradients.

REFERENCES

[1] Prandoni, I., "The sardinia radio telescope: From a technological project to a radio observatory," *Astronomy Astrophysics* **608**, A40 (2017).

[2] Buffa, F., Serra, G., and Poppi, S., "Hop user guide," *OAC - Internal Report* **71** (2018).

[3] Nikolic, B., Hills, R., and Richer, J., "Measurement of antenna surface from in- and out-of-focus beam maps using astronomical sources," *Astronomy Astrophysics* **456**, 679–683 (2007).

[4] Jian, D., Weiye, Z., Jinqing, W., Qinghui, L., and Zhiqiang, S., "Correcting gravitational deformation at the tianma radio telescope," *IEEE Transactions on Antennas and Propagation* **66**, 2044–2048 (2018).

[5] Melis, A., Concu, R., Trois, A., and Possenti, A., "Sardinia roach2-based digital architecture for radio astronomy (sardara)," *Journal of Astronomical Instrumentation* **07** (2018).

[6] Suss, M., Koch, D., and Paluszek, H., "The sardinia radio telescope (srt) optical alignmen," *Proc. SPIE8444 Ground-based and Airborne Telescopes IV* **84442G** (2012).